Designing 'Totem' C_2-Symmetrical Iron Porphyrin Catalysts for Stereoselective Cyclopropanations

Daniela Maria Carminati,[a] Daniela Intrieri,[a] Alessandro Caselli,[a] Stéphane Le Gac,[b] Bernard Boitrel,*[b] Lucio Toma,*[c] Laura Legnani[c] and Emma Gallo*[a]

Abstract: The catalytic activity of the iron(III) C_2 chiral porphyrin Fe(**2**)(OMe) in the alkene cyclopropanation is herein reported. The catalyst promoted the reaction of differently substituted styrenes with diazo derivatives with *trans*-diastereoselectivities and enantioselectivities up to 99:1 and 87%, respectively. In addition, high TON and TOF values (up to 10,000 and 120,000 h^{-1}, respectively) were observed indicating good activity and stability of the catalyst in optimised experimental conditions. The study of the cyclopropanation reaction revealed that the porphyrin skeleton is composed of two '*totem*' parts which were independently responsible for the observed enantio- and diastereoselectivities. To further our research we also investigated the catalytic role of the methoxy axial ligand coordinated to the iron atom. The molecular structure of Fe(**2**)(OMe) was optimised by DFT calculations which were also employed to achieve mechanistic details of the carbene transfer reaction.

Introduction

The ring strain of cyclopropanes furnishes them with a number of interesting peculiarities which are crucial when using this class of molecules as pharmaceutical and/or biological agents[1-6] as well as versatile building blocks in organic synthesis.[5, 7-9] Consequently, the interest of the scientific community in developing new protocols to obtain these compounds is growing[10, 11] and great efforts have been made to fine-tune the eco-compatibility of the processes to respect social requests for a sustainable synthetic chemistry. In this context, the cyclopropane synthesis by the metal-catalysed one-pot reaction of diazo compounds with alkenes represents a valuable synthetic strategy thanks to the formation of benign molecular nitrogen as the only stoichiometric by-product of the carbene transfer reaction.[12-16]

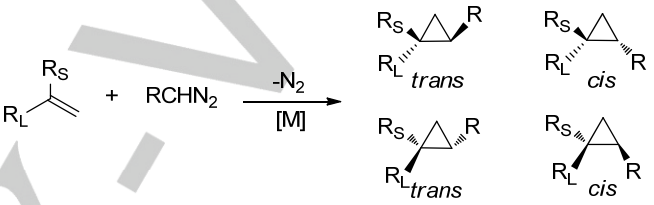

Scheme 1. Metal-catalysed one-pot reaction of diazo compounds with alkenes.

Note that the eco-tolerability of cyclopropanation reactions can be further enhanced by i) using continuous flow methodologies due to the safe handling of hazardous reagents such as diazo compounds,[17-20] ii) applying biomimetic catalysts coupling a very good catalytic activity with a natural high chemical selectivity[21-26] and iii) employing unconventional catalytic systems such as supramolecular cage catalysts which simulate the working operandi of enzymes.[27-30]

Amongst all the metal catalysts, metal porphyrins were very active and ruthenium,[31-34] osmium,[35, 36] rhodium[37-39] and iridium[40] porphyrin complexes have been extensively employed to promote cyclopropanation reactions. In spite of the good catalytic efficiency of the above mentioned porphyrin catalysts, their high cost and toxicity prompted the study of the more eco-friendly first row transition metal porphyrins, such as cobalt[41-46] and iron[47-54] derivatives. Cobalt(II) porphyrins were largely employed in the stereoselective synthesis of cyclopropanes with excellent results,[42, 55-57] which were also attributed to a synergistic action of the active metal centre with the ligand periphery. It was described that the insertion of opportune functional groups onto the porphyrin skeleton can be fundamental to correctly drive the reaction of the carbene intermediate with the double bond of the alkene. Concerning iron porphyrin complexes, they have been extensively employed in oxygenation catalysis and their first use in cyclopropanation was reported in 1999 by S. Gross and co-workers.[58] Since then, numerous iron porphyrin complexes have been synthesised to be applied to carbene transfer reactions and several structural modifications of the ligand skeleton have been performed to

[a] D. M. Carminati, Dr. D. Intrieri, Prof. A. Caselli, Prof. E. Gallo
Department of Chemistry, University of Milan
Via C. Golgi 19, 20133 Milan (Italy)
E-mail: emma.gallo@unimi.it
[b] Dr. S. Le Gac, Dr. B. Boitrel
Institut des Sciences Chimiques de Rennes, Université de Rennes 1
263 avenue du Général Leclerc, 35042 Rennes Cedex (France)
[c] Prof. L. Toma, Dr. L. Legnani
Department of Chemistry, University of Pavia
Via Taramelli 12, 27100 Pavia (Italy)

Supporting information for this article is given via a link at the end of the document.

afford a catalyst whose efficiency could be maximised by a metal/periphery synergy.[59]

In accord with this approach, we have investigated the employment of "non innocent ligands" such as *bis*-strapped porphyrins[60-66] which, thanks to the presence of 5-15 bridging in the skeleton, permits the insertion of appropriate functionalised groups close to the active site. We have recently communicated the functionalization of porphyrin **1**[67] with (*R*)-(2,2'-dimethoxy-[1,1'-binaphthal-ene]-3,3'-diyl)diboronic acid by a $(Ph_3P)_4Pd$-catalysed Suzuki coupling reaction forming the new chiral *bis*-strapped porphyrin **2** (Scheme 2).[68]

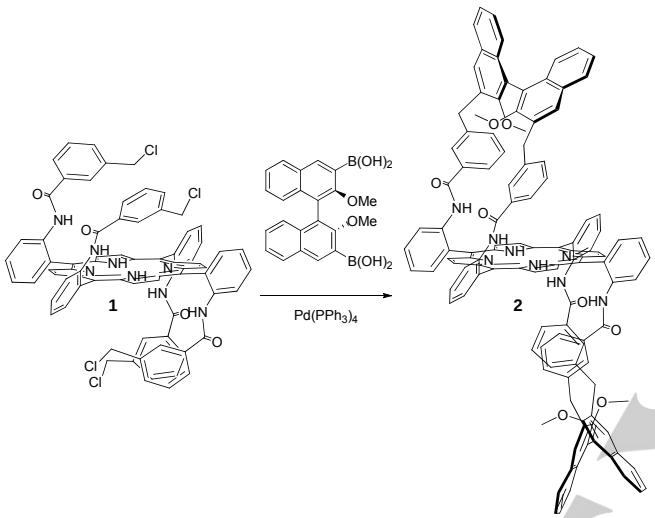

Scheme 2. Synthesis of the chiral *bis*-strapped porphyrin **2**.

Porphyrin **2** was fully characterised and reacted with $FeBr_2$ to first yield an iron(II) species which was oxidised by the atmospheric oxygen in the presence of MeOH to form iron(III) Fe(**2**)(OMe) complex in a quantitative yield. Complex Fe(**2**)(OMe) was fully characterised and tested as the catalyst of the cyclopropanation of α-methylstyrene by ethyl diazoacetate (EDA) which occurred with excellent stereoselectivity, TON and TOF.

In view of the good quality of the achieved results we further investigated the catalytic activity of Fe(**2**)(OMe) complex and we herein present the study of the reaction scope performed by testing the reactivity of several diazo compounds towards differently substituted alkenes. In addition, the influence of the three dimensional *bis*-strapped porphyrin ligand on the iron catalyst performance was investigated from both experimental and theoretical points of view.

Results and Discussion

Catalytic data. The optimisation of the Fe(**2**)(OMe)-catalysed cyclopropanation of α-methylstyrene indicated that best catalytic performances were observed by performing the cyclopropanation reaction in toluene at 0°C by using a slight excess of EDA.[68] Then, we started the study of the reaction scope by testing the reactivity of several alkenes towards EDA and achieved data have been collected in Table 1.

As reported in Table 1, six of the eleven tested substrates reacted at 25°C by using either the equimolar ratio alkene/EDA =1000:1000 (Table 1, entries 1,6,11,16,29 and 33) or a slight EDA excess (Table 1, entries 2,7,12,17,30 and 34). It is worth noting that all the reactions were performed without using an alkene excess which can be a drawback if expensive alkenes are the reagents of choice. The increase of cyclopropane yields, registered when the alkene/EDA ratio of 1000:1100 was used (see below for a probable explanation of this effect), prompted us to apply this catalytic ratio at lower temperatures to optimise the reaction stereoselectivity. The synthesis of cyclopropanes **3**-**13** was executed at 0°C and -40°C where enantioselectivities up to 87% were registered with a contemporary increase of the reaction times. It is interesting to note that the *trans*-diastereoselectivity was almost independent from the employed experimental conditions and, except for the synthesis of compound **10**, the *trans*/*cis* ratio was larger than 90:10. Reaction diastereoselectivities and yields were both influenced by the steric hindrance of unsaturated substrates. Best results were obtained for the cyclopropanation of $Ar(R)C{=}CH_2$ substrates where R is a methyl group and when the methyl group was replaced by a hydrogen atom a general decrease of the reaction efficiency occurred (Table 1, compare entries 9 and 14). A further increase of the steric hindrance of the R group was not responsible for an increase of the reaction efficiency and when the methyl group was substituted by a phenyl group a modest yield and stereoselectivity were observed (Table 1, compare entries 4 and 32). Also the steric hindrance of the aryl group on the alkene was crucial in determining good catalytic outcomes and the synthesis of compound **12**, where Ar = binaphtyl, occurred with modest yields and enantioselectivities at all tested temperatures (Table 1, entries 40, 41 and 42). It should be noted that the cyclopropanation of (1*S*)-β-pinene occurred with a good stereospecificity and only two of the four possible diasteroisomers were detected. The major diasteromer was isolated and the absolute configuration of 1*R*,2*R*,2'*R* was attributed by comparing achieved data with those reported in literature for the pure compound.[69]

The substrates which revealed the best reactivity were also tested at 0°C by using the catalytic ratio Fe(**2**)(OMe)/alkene/EDA = 1:10000:10100. Good catalytic results were achieved by using the low catalytic loading of 0.01% (TON = 10,000) (Table 1, entries 5, 10, 15, 20, 24 and 28) to validate the huge chemical stability/activity relationship of the employed iron catalyst. It should be underlined that the reaction time was very short in several cases and in the cyclopropanation of α-methylstyrene the reaction occurred in 5 minutes affording an excellent value of TOF equal to 120,000 h^{-1}.

Table 1. Fe(**2**)(OMe)-catalysed cyclopropanation of alkenes by EDA to form compounds **3**-**13**.[a]

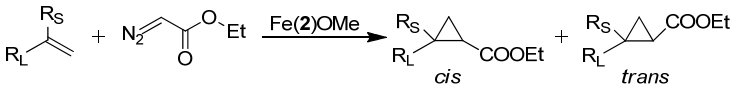

entry	alkene	cat/alkene/EDA	T (°C)	t (min)[b]	product, (%)[c]	yield$_{trans}$	*trans*/*cis*[d]	*ee*$_{trans}$ (%)[e]
1		1:1000:1000	25	5	**3**, 75		97:3	68
2		1:1000:1100	25	5	**3**, 85		98:2	70
3		1:1000:1100	0	5	**3**, 76		98:2	69
4		1:1000:1100	-40	15	**3**, 98		98:2	87
5		1:10000:10100	0	5	**3**, 98		96:4	76
6	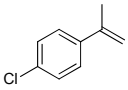	1:1000:1000	25	10	**4**, 65		97:3	67
7		1:1000:1100	25	5	**4**, 84		95:5	76
8		1:1000:1100	0	15	**4**, 80		99:1	80
9		1:1000:1100	-40	20	**4**, 80		99:1	80
10		1:10000:10100	0	30	**4**, 80		97:3	70
11	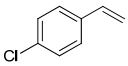	1:1000:1000	25	5	**5**, 40		97:3	36
12		1:1000:1100	25	5	**5**, 60		95:5	28
13		1:1000:1100	0	5	**5**, 65		97:3	41
14		1:1000:1100	-40	15	**5**, 60		98:2	60
15		1:10000:10100	0	20	**5**, 62		97:3	57
16	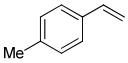	1:1000:1000	25	5	**6**, 60		95:5	35
17		1:1000:1100	25	5	**6**, 65		95:5	34
18		1:1000:1100	0	15	**6**, 72		98:2	50
19		1:1000:1100	-40	15	**6**, 72		99:1	68
20		1:10000:10100	0	15	**6**, 53		97:3	64
21	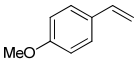	1:1000:1100	25	5	**7**, 65		95:5	50
22		1:1000:1100	0	10	**7**, 72		97:3	61
23		1:1000:1100	-40	20	**7**, 72		99:1	60
24		1:10000:10100	0	30	**7**, 74		95:5	60
25	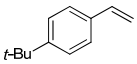	1:1000:1100	25	5	**8**, 60		94:6	38
26		1:1000:1100	0	15	**8**, 70		95:5	43
27		1:1000:1100	-40	15	**8**, 85		98:2	63
28		1:10000:10100	0	5	**8**, 70		98:2	40
29		1:1000:1000	25	5	**9**, 34		-	2
30		1:1000:1100	25	5	**9**, 33		-	2
31		1:1000:1100	0	35	**9**, 34		-	5
32		1:1000:1100	-40	120	**9**, 25		-	48
33		1:1000:1000	25	5	**10**, 23		81:19[f]	-
34		1:1000:1100	25	5	**10**, 28		82:18[f]	-
35		1:1000:1100	0	5	**10**, 26		84:16[f]	-
36		1:1000:1100	-40	60	**10**, 20		97:3[f]	-
37	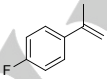	1:1000:1100	25	60	**11**, 46		95:5	65
38		1:1000:1100	0	120	**11**, 30		90:10	64
39		1:1000:1100	-40	120	**11**, 30		91:9	71
40	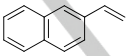	1:1000:1100	25	60	**12**, 45		95:5	42
41		1:1000:1100	0	60	**12**, 40		97:3	37
42		1:1000:1100	-40	90	**12**, 45		97:3	40
43	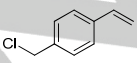	1:1000:1100	25	15	**13**, 45		99:1	n.d.
44		1:1000:1100	0	70	**13**, 50		99:1	n.d.
45		1:1000:1100	-40	90	**13**, 60		98:2	n.d.

[a] The opportune Fe(**2**)(OMe) (1.0 mL of 5.40 x 10^{-4} mol/L toluene solution)/alkene/EDA ratio was dissolved in 2.0 mL of toluene. [b] Time required for the EDA conversion monitored by IR spectroscopy. [c] Isolated yield of the *trans* isomer; beside the *cis* isomer, coupling by-products derived from EDA accounted for the reaction mass balance. [d] Diastereomeric ratio determined by ^{1}H NMR analysis of the crude before the isolation of the *trans* major isomer. No attempts were made to isolate the *cis* isomer. [e] Enantiomeric excess of the *trans*(*R*,*R*) major diasteromer determined by HPLC analysis (see SI). [f] Only two diasteromers were detected. The absolute configuration of the major isomer was 1*R*,2*R*,2'*R*.

To better study the reaction scope, α-methylstyrene was chosen as the unsaturated substrate to test the reactivity of other diazo derivatives. Collected data reported in Table 2 indicated that the catalytic efficiency strongly depended on the steric hindrance of the R substituent of $(RO_2C)CH=N_2$ diazo reagent. The stereoselectivity of the reaction was acceptable with R = ethyl (Table 2, entry 1, compound **3**) and R = ^{i}propyl (Table 2, entry 2, compound **14**) but, even if the diastereoselectivity of the cyclopropanation by using (^{n}PrO$_2$C)CH=N$_2$ (Table 2, entry 3, compound **15**) was very high, a drastic decrease in the reaction enantioselectivity was observed. This trend was confirmed by employing (^{t}BuO$_2$C)CH=N$_2$ as the diazo reagent where a modest diastereoselectivity and a very low enantioselectivity were registered (Table 2, entry 4, compound **16**). This result is in accord with the reported statement that an increase of the diazoacetate size could provoke a decrease of the reaction enantioselectivity using the same catalyst.[70]

Table 2. Fe(**2**)(OMe)-catalysed cyclopropanation of α-methylstyrene by $(RO_2C)CH=N_2$[a]

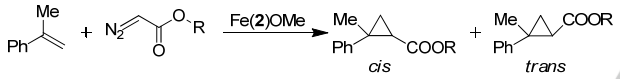

entry	R	t (min)[b]	product, (%)[c]	yield$_{trans}$	*trans*/*cis*[d]	*ee*$_{trans}$ (%)[e]
1	Et	5	**3**, 85		98:2	70
2	^{i}Pr	120	**14**, 60		98:2	67
3	^{n}Pr	90	**15**, 73		98:2	40
4	^{t}Bu	120	**16**, 42		63:37	7

[a] Fe(**2**)(OMe) (1.0 mL of 5.40 x 10^{-4} mol/L toluene solution)/α-methylstyrene/diazo compound = 1:1000:1100 in 2.0 mL of toluene at 25°C. [b] Time required for the diazo compound conversion monitored by IR spectroscopy. [c] Isolated yield of the *trans* isomer; beside the *cis* isomer, coupling by-products derived from diazo reagent accounted for the reaction mass balance. [d] Diasteromeric ratio determined by ^{1}H NMR. [e] Enantiomeric excess of the *trans*(*R,R*) major diastereomer determined by HPLC analysis (see SI for experimental details).

When α-methylstyrene was treated with more sterically hindered diazo reagents such as benzyl 2-diazoacetate, $(PhCH_2O_2C)CH=N_2$, 1–phenylpropan-2-yl-diazoacetate, $(PhCH_2(Me)CHO_2C)CH=N_2$ or ethyl 2-diazo-3-oxobutanoate, $(EtO_2C)(MeOC)C=N_2$ the cyclopropanation was inhibited. It can be suggested that the iron centre, placed in a crowded porphyrin structure, cannot interact with these diazo derivatives for steric reasons and consequently the carbene transfer reaction to the alkene does not occur.

In order to better explore what has been stated above, precursor porphyrin **1** was employed to synthesise Fe(**1**)(OMe) which lacks the two chiral binaphthyl moieties thus resulting in a decrease of the steric bulk surrounding the porphyrin core. Complex Fe(**1**)(OMe) was obtained in a quantitative yield by using the same procedure employed to synthesise Fe(**2**)(OMe)[68] and fully characterised. The MS-ESI analysis showed the presence of the methoxy ligand and the ESR spectroscopy established the oxidation state of the iron(III) metal centre with S = 5/2. Complex Fe(**1**)(OMe) was then used to catalyse the synthesis of cyclopropanes **3**-**18** reported in Table 3.

As reported in Table 3, the reaction diastereoselectivities observed in the presence of Fe(**1**)(OMe) were comparable to those reported above for cyclopropanations promoted by Fe(**2**)(OMe) to indicate a similar tridimensional arrangement for the two porphyrin catalysts. In addition, the reactions occurred with analogous times and yields. A fundamental difference between the two catalysts was observed in the cyclopropanation of α-methylstyrene by sterically hindered diazo compounds. The reaction between *tert*-butyl diazo acetate and α-methylstyrene catalysed either by Fe(**1**)(OMe) (Table 3, entry 4) or Fe(**2**)(OMe) (Table 2, entry 4) occurred with a better yield and diastereoselectivity in the presence of the less hindered Fe(**1**)(OMe) pointing out a dependence of the catalytic efficiency on the degree of the steric bulk close to the porphyrin plane. The divergence between the Fe(**1**)(OMe) and Fe(**2**)(OMe) catalytic behaviour was enhanced by increasing the steric hindrance of the employed diazo starting reagent. Whilst no reaction was observed between benzyl 2-diazoacetate and α-methylstyrene in the presence of Fe(**2**)(OMe), cyclopropane **17** was formed with an acceptable yield of 45% and good *trans* diastereoselection of 91:9 when the reaction was catalysed by Fe(**1**)(OMe) (Table 3, entry 5). Complex Fe(**1**)(OMe) was also active in promoting the reaction of α-methylstyrene with the very sterically hindered 1-phenylpropan-2-yl-diazoacetate (Table 3, entry 6) where, even if the cyclopropanation occurred in a long reaction time and **18** was formed in a low yield, the good *trans*/*cis* ratio of 94:6 was observed. Complex Fe(**1**)(OMe) was also used at the very low catalyst loading of 0.01% where compounds **3**-**8** were obtained in reasonable yields and short reaction times (Table 3, entries 7, 9, 11, 13, 15, 17). In particular, cyclopropane **3** was formed with the outstanding TON and TOF values of 10,000 and 120,000 respectively (Table 3, entry 7). For all the other substrates TOF values larger than 60,000 were observed.

Data reported on the catalytic activity of Fe(**1**)(OMe) suggested that the excellent diastereoselectivities induced by the *bis*-strapped chiral porphyrin Fe(**2**)(OMe) can be principally ascribed to the portion of the porphyrin skeleton which does not include the binaphthyl part. This important result paves the way for a wide use of Fe(**1**)(OMe) as a precursor of a large class of chiral catalysts. In fact, the benzylic groups of the two arms of porphyrin **1** can be functionalised with various chiral groups to obtain a small library of structurally different chiral catalysts whose activity in inducing a reaction diastereoselectivity is independent from the steric nature of the chiral group.

Table 3. Fe(**1**)(OMe)-catalysed cyclopropanation of alkenes by EDA to form compounds **3**-**18**.[a]

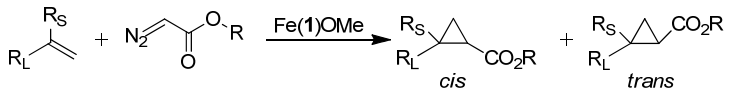

entry	alkene	cat/alkene/EDA	R	t (min)[b]	product, yield (%)[c]	*trans*/*cis*[d]
1		1:1000:1100	ethyl	5	**3**, 80	92:8
2		1:1000:1100	*i*propyl	20	**14**, 65	95:5
3		1:1000:1100	*n*propyl	60	**15**, 72	90:10
4		1:1000:1100	*t*buthyl	15	**16**, 60	97:3
5		1:1000:1100	benzyl	15	**17**, 45	91:9
6		1:1000:1100	1-phenylpropan-2-yl	240	**18**, 35	94:6
7		1:10000:10100	ethyl	5	**3**, 68	91:9
8	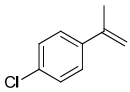	1:1000:1100	ethyl	10	**4**, 60	91:9
9		1:10000:10100	ethyl	5	**4**, 57	98:2
10	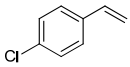	1:1000:1100	ethyl	20	**5**, 40	97:3
11		1:10000:10100	ethyl	10	**5**, 37	95:5
12	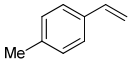	1:1000:1100	ethyl	5	**6**, 78	94:6
13		1:10000:10100	ethyl	5	**6**, 52	97:3
14	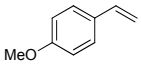	1:1000:1100	ethyl	10	**7**, 75	90:10
15		1:10000:10100	ethyl	10	**7**, 70	89:11
16	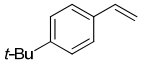	1:1000:1100	ethyl	5	**8**, 80	94:6
17		1:10000:10100	ethyl	5	**8**, 75	94:6
18		1:1000:1100	ethyl	5	**9**, 56	-
19		11:1000:1100	ethyl	60	**10**, 32	82:18[e]
20	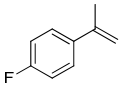	1:1000:1100	ethyl	60	**11**, 43	92:8
21	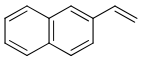	1:1000:1100	ethyl	60	**12**, 57	91:9
22	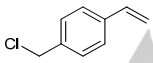	1:1000:1100	ethyl	60	**13**, 75	94:6

[a] The opportune Fe(**1**)(OMe)(1.0 mL of 5.40 x 10^{-4} mol/L toluene solution)/alkene/diazo compound ratio was dissolved in 2.0 mL of toluene. [b] Time required for diazo compound conversion monitored by IR spectroscopy [c]. Isolated yield of the *trans* isomer; beside the *cis* isomer, coupling by-products derived from the diazo reagent accounted for the mass balance of the reaction. [d] Diastereomeric ratio determined by ^{1}H NMR analysis of the crude before the isolation of the *trans* mayor isomer. No attempts were made to isolate the *cis* isomer.

Catalyst Recycle and Recover. In a previously reported communication the catalytic robustness of Fe(**2**)(OMe) was tested by repeating the cyclopropanation of α–methylstyrene by EDA for three consecutive times.[68] The opportune amounts of reagents were added to the catalytic mixture under nitrogen and 90% of global yield, 98:2 of *trans*-diastereoselectivity and 75% of ee_{trans} were achieved to reveal a good catalyst recyclability when the mixture was kept under an inert atmosphere. In order to also

evaluate the catalyst recycle in a non-protected reaction medium, the experiment described above was repeated but after every run the catalytic mixture was evaporated to dryness, left standing in open air and analysed to evaluate the chemo- and stereoselectivity after each catalytic run. Every successive run was performed in dry toluene under nitrogen by using the catalytic Fe(**2**)(OMe)/α-methylstyrene/EDA ratio of 1:1000:1000. After the first run, where the cyclopropanation of α-methylstyrene occurred in 5 minutes in 72% yield, 94:2 of *trans*-diastereoselectivity and 77% ee_{trans}, a decrease of the chemoselectivity was observed. The analysis of the reaction crude after the second run revealed that compound **3** was still formed with a good stereoselectivity (*trans*/*cis* = 98:2 and 75% ee_{trans}) but the low yield of 38% indicated a decrease of the catalytic efficiency. Then, when the reaction was repeated for the third time the desired cyclopropane was obtained only in traces to point out that a catalyst deactivation took place.

Considering the catalytic positive effect of the EDA excess (see above), we repeated the sequence of the three catalytic reactions by replacing the Fe(**2**)(OMe)/α-methylstyrene/EDA ratio of 1:1000:1000 with 1:1000:1100. By using an EDA excess the three runs occurred with similar chemo- and stereoselectivities; in the first run the cyclopropane **3** was obtained in 5 minutes, at a 76% yield, 97:3 of *trans*-diastereoselectivity and 70% ee_{trans}; in the second run the cyclopropane formation was achieved in 10 minutes, 77% yield, 95:5 of *trans*-diastereoselectivity and 78% ee_{trans} and finally, in the last run compound **3** was formed after 10 minutes with 90% yield, 98:2 of *trans*-diastereoselectivity and 73% ee_{trans}. This last experiment proved that the EDA excess was fundamental to assure a good recycle of the catalyst by avoiding degradation pathways of the active species due to the presence of air.

Considering the deactivation role of air traces, we decided to separately investigate the influence of molecular oxygen and water on the catalytic performance of Fe(**2**)(OMe) in promoting the reaction between equimolar amounts of α-methylstyrene and EDA. When the reaction was run in air by using a flask equipped with a calcium chloride drying tube, cyclopropane **3** was formed after 10 minutes in 78% yield with 98:2 of *trans*-diastereoselectivity and 65% ee_{trans}. A similar result was obtained by running the model reaction in air but in the presence of activated molecular sieves where **3** was formed in 64% yield with 97:3 of diastereoselectivity and 75% ee_{trans}. It is important to note that achieved data were comparable to those collected when the synthesis of **3** was performed under nitrogen atmosphere (Table 1, entry 1).

Conversely, if the reaction was carried out under nitrogen but in a wet toluene, obtained by adding 0.03% of degassed water to a dried solvent, the cyclopropanation only occurred partially and **3** was formed in the low yield of 12% but still good diastereo- and enantioselectivities were observed (99:1 of *trans*-diastereoselectivity, 71% ee_{trans}). This result suggested that the catalytic process inhibition, observed when the reaction mixture was exposed for a short period of time to air, was mainly due to the presence of humidity rather than to oxidative side reactions. In order to better investigate the role of the water in the catalytic reactions, we also analysed the stability of Fe(**2**)(OMe) in a wet solvent by leaving the catalyst to stand in toluene containing 0.03% of water for 24 h in toluene, after which the obtained solution was evaporated to dryness and the residue analysed by ESI-MS. The resulting spectrum disclosed the partial conversion of Fe(**2**)(OMe) into Fe(**2**)OH and the identity of the latter complex was confirmed by comparing achieved data with those relative to pure Fe(**2**)OH synthesised by reacting porphyrin **2** first with $FeBr_2$ and then with NaOH (see Experimental Section). The so-obtained Fe(**2**)OH was fully characterised and tested as a catalyst of the model reaction between α-methylstyrene and EDA. Complex Fe(**2**)OH showed a poor catalytic activity suggesting an important role of the methoxy ligand to mediate the carbene transfer reaction.

All data reported up to now indicated that traces of humidity in the catalytic reaction were responsible for the formation of the less catalytic active Fe(**2**)OH (Scheme 3, *path* a) and then, an EDA excess was required to favour the catalytic productive *path b* responsible for the formation of the putative terminal (**X**) or bridging (**Y**) active carbene species (Scheme 3).

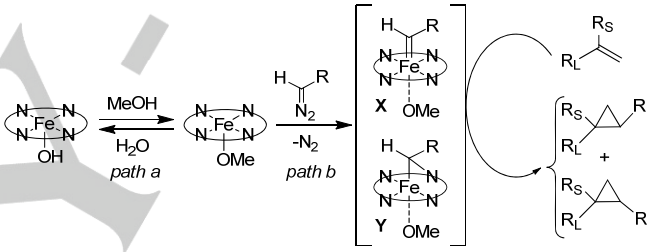

Scheme 3. Mechanistic proposal for Fe(**2**)(OMe)-catalysed cyclopropanation.

It is important to note that the formation of Fe(**2**)OH was not an irreversible process and the active catalyst Fe(**2**)(OMe) was easily restored by stirring Fe(**2**)OH in dried MeOH for 10 hours at room temperature. The formation of Fe(**2**)(OMe) was confirmed by ESI-MS analysis and the restored catalyst was active in promoting the synthesis of cyclopropane **3** which was obtained with 67% yield, 96:4 of *trans*-diastereoselectivity and 70% ee_{trans}.

To expand the exploration of the catalytic role of the methoxy ligand, we performed a cyclopropanation reaction using 8.0 mg of Fe(**2**)(OMe) catalyst in 25.0 mL of toluene (cat/α-methylstyrene/EDA = 1:1000:1100) and the ESI-MS analysis of the crude after the reaction completion revealed the presence of Fe(**2**)(OMe) together with cyclopropane products and small amounts of other unidentified iron porphyrin complexes. The detection of Fe(**2**)(OMe) complex indicated that although, the initial iron(III) catalyst was reduced by EDA to an iron(II) species before reacting with the diazo reagent to form an active iron(IV) carbene intermediate, as already reported,[48, 71] the methoxy axial ligand was retained during the catalytic reaction and could have influenced the catalytic performance. On the other hand, it can be also envisaged that the starting iron(III) Fe(**2**)(OMe) species was directly transformed into a carbene intermediate without its preliminary reduction to an iron(II) complex. This second hypothesis can be supported by

the efficiency of the **2**-catalysed cyclopropanation of α-methylstyrene by EDA in the presence of molecular oxygen (see above). It is important to remind that when an iron(II) species is involved in the catalytic cycle, the reaction is completely inhibited by the presence of air.[48]

All attempts to isolate and/or spectroscopically observe the active carbene iron species **X** or **Y** (Scheme 3) have failed up to now probably due to the well-known chemical instability of *mono*-substituted 'M=CHR' carbene complexes which can be very easily involved in degradation processes.[54]

Considering that experimental collected data are not conclusive to suggest a reaction mechanism, *path b* of Scheme 3 was postulated on the basis of other reported studies.[48, 72-74] Then, the interaction of the elusive carbene intermediate **X** or **Y** with the approaching alkene, which is responsible for the cyclopropane formation, was studied from a theoretical point of view as illustrated in the following section.

DFT Theoretical Studies. Considering the influence of the tridimensional structure of the porphyrin skeleton on the reaction diastereo- and enantioselectivity, a DFT study was performed to better analyse the properties of catalysts Fe(**1**)(OMe) and Fe(**2**)(OMe). Calculations were performed, using the Gaussian09 package,[75] first on free ligands at the B3LYP[76, 77] level with the 6-31G(d) basis set and then on their iron complexes using the same basis set for all atoms except the effective core potential LanL2DZ basis set used for iron.

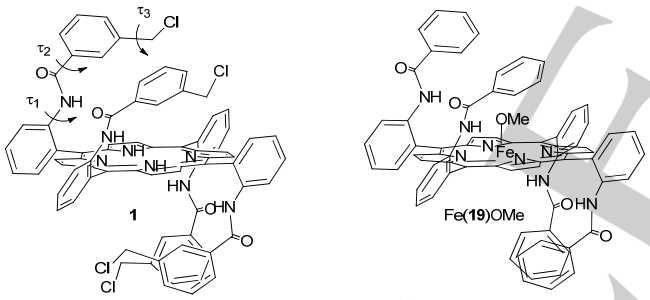

Chart 1. Structures of porphyrin **1** and Fe(**19**)(OMe) complex.

Though simpler than **2** and hence easier to study, the geometrical analysis of porphyrin **1** is quite complex as it shows several degrees of conformational freedom deriving from the various orientations that the pickets can assume and corresponding to different values of the torsional angles τ_1, τ_2, and τ_3 (Chart 1). Tens of minimum energy conformers were obtained after the optimization of all the predictable molecular geometries, a dozen of which in a range of 2.5 kcal/mol above the global minimum. Figure 1 reports the three-dimensional plots of the two most stable conformers which exemplify their main geometrical features. The phenyl groups of the pickets can assume an almost orthogonal arrangement, as in **1A**, with one phenyl above or below the porphyrin ring and the other at one side of the system, or an arrangement, as in **1B**, with an angle of about 30° between the planes of the phenyls that leave an empty space above and below the porphyrin plane. A large variability can be observed for the orientation of the chloromethyl groups that can occupy one or the other *meta*-position with the CH_2-Cl bond perpendicular to the phenyl plane and assuming an external or internal orientation, thus making possible four different chloromethyl orientations for each phenyl group.

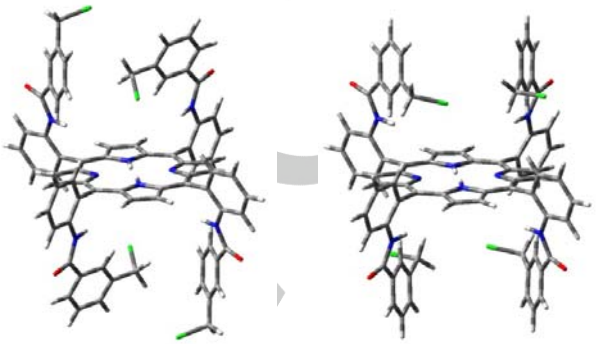

1A (0.00) **1B** (0.11)

Figure 1. Three-dimensional plots of the preferred conformers of porphyrin **1** (relative energy values, kcal/mol, in parentheses).

Then, the influence of the central iron metal and the methoxy ligand on the geometrical preferences of **1** had to be determined. However, the very high number of conformers of **1** made almost impracticable a complete conformational evaluation of Fe(**1**)(OMe). So, taking into account that, in spite of the large variability in the orientation of the chloromethyl groups, the relative orientation of the pickets are only the two ones represented in Figure 1, a simplified model, Fe(**19**)(OMe) (Chart 1), was evaluated. This paramagnetic complex was modeled at the unrestricted UB3LYP level, minimizing the energy of all the predictable geometries based on the located conformers of **1** modified by introduction of iron and the methoxy group. The optimizations were performed on the Fe(**19**)(OMe) conformers in doublet (S =1/2), quartet (S = 3/2), and sextet (S = 5/2) states. The high spin sextet state was energetically favoured in agreement to experimental magnetic measurements obtained for complexes Fe(**1**)(OMe) and Fe(**2**)(OMe) (see above and experimental section).

The methoxy group of Fe(**19**)(OMe) occupies the space that phenyls leave empty so that, in correspondence of each orientation of the phenyls of the pickets, a precise methoxy orientation was observed. In conformer Fe(**19**)(OMe)-**A** the methoxy methyl group is away from the phenyls whereas in conformer Fe(**19**)(OMe)-**B** it is placed between them (Figure 2). Conformer Fe(**19**)(OMe)-**A** was found to be the global minimum being more stable than Fe(**19**)(OMe)-**B** by 1.61 kcal/mol. Conformer Fe(**19**)(OMe)-**A** in the lower quartet and doublet states showed an energy higher by about 2 and 5 kcal/mol, respectively.

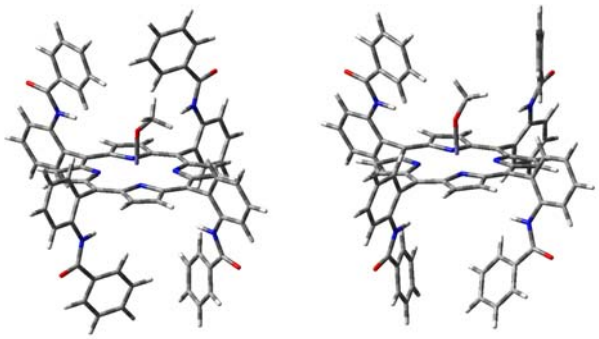

Fe(**19**)(OMe)-**A** (0.00) Fe(**19**)(OMe)-**B** (1.61)

Figure 2. Three-dimensional plots of the preferred conformers of the model Fe(**19**)(OMe) complex (relative energy values, kcal/mol, in parentheses).

The conformational preferences of the ligand **2** were then investigated and the study started from the simplified single-binaphthyl-handled porphyrin **20** shown in Chart 2. In principle, the presence of benzyl groups in the pickets and the binaphthyl moiety connecting them should confer a certain rigidity to the structure. However, several single bonds are present, i.e. those connecting the *meso*-phenyls to the amido groups and these to the benzene rings, as well as the two single C-C bonds of the methylenes that link the benzene rings to naphthalenes. All of them represent degrees of conformational freedom (τ_1-τ_4, Chart 2) that can combine in a significant number of different geometries that were built and optimized. A particular fold resulted largely preferred, represented by the four most stable conformers **20A**-**D** (Figure 3), whereas the other folds resulted much less stable (Figure 1S, SI). It is worthy pointing out that the main differences among **20A**-**D** consist in the orientation of the naphthyl methoxy groups and in the distance between the phenyls of the pickets that are closer in **20A** than in **20B**-**D**. These four conformers are readily interchangeable, the resulting effect being an enlargement or a shrinking of the empty space between the phenyls, thus determining the possibility for the cavity to accommodate axial ligands or guests of suitable sizes.

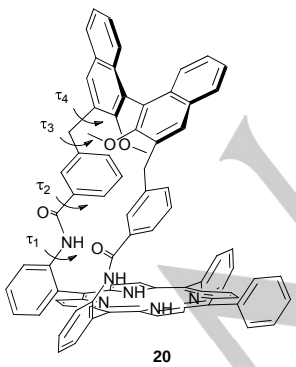

20

Chart 2. Structure of the model single-binaphthyl-handled porphyrin **20**.

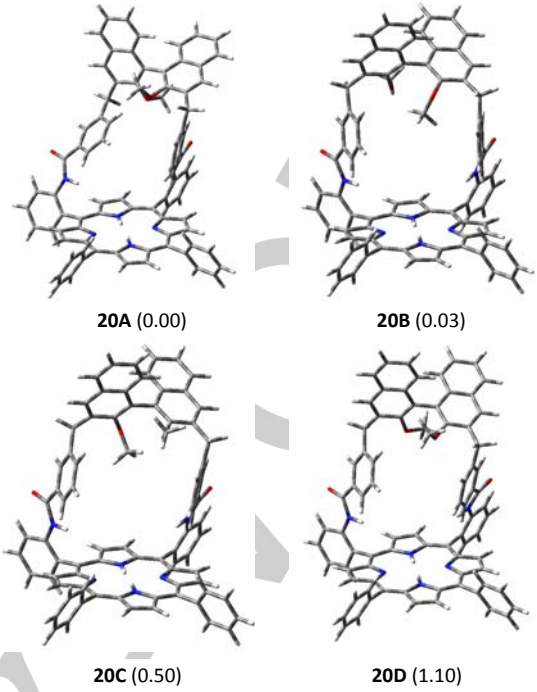

20A (0.00) **20B** (0.03)

20C (0.50) **20D** (1.10)

Figure 3. Three-dimensional plots of the preferred conformers of the model single-binaphthyl-handled porphyrin **20** (relative energy values, kcal/mol, in parentheses).

The second handle was then added to the structure to obtain the entire ligand **2**. No noteworthy difference was observed in the conformational behaviour of **2** with respect to **20** as conformers **2A**-**D**, located as the most stable ones, faithfully reproduce the geometrical features of the corresponding conformers of **20** (Figure 2S, SI). For this reason, all the following data are referred to single-binaphthyl-handled structures, thus making possible to perform shorter calculations without losing significant information.

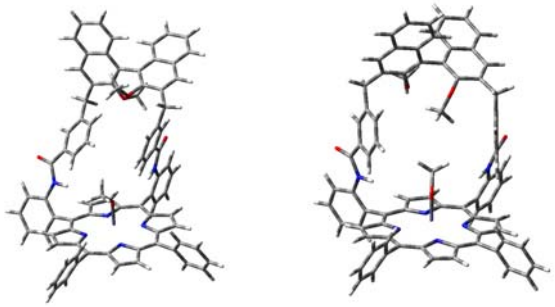

Fe(**20**)(OMe)-**A** (0.00) Fe(**20**)(OMe)-**B** (0.61)

Figure 4. Three-dimensional plot of the preferred conformers of the Fe(**20**)(OMe) complex (relative energy values, kcal/mol, in parentheses).

The Fe(**20**)(OMe) complex in the sextet state (S = 5/2) was so modelled and, as in the case of Fe(**19**)(OMe), the axial methoxy ligand orients the methyl group towards a *meso*-carbon atom as shown in Figure 4 that reports the two preferred conformers of the Fe(**20**)(OMe) complex corresponding to the **20A** and **20B** conformers of **20**.

As reported above, active carbene species (**X,** *terminal* and **Y**, *bridging,* Scheme 3), generated by the reaction of EDA with the iron (III) methoxy complexes are supposed to be the intermediates in the iron catalyzed cyclopropanation reactions. The geometrical and electronic features of such intermediates are of utmost importance in driving the possible reaction paths towards the observed selectivity. In order to investigate the mechanism of the stereocontrol observed for Fe(**1**)(OMe) and Fe(**2**)(OMe) catalysed cyclopropanations, it is important to determine their preferred spin state as well as to define the carbene binding mode which can be *bridging*, when the carbene carbon atom is linked to both iron and a porphyrin nitrogen atom (**Y**, Scheme 3), or *terminal*, if a double Fe=$C_{carbene}$ bond is present in the structure (**X**, Scheme 3).

It should be noted that all calculations reported herein refer to the spin state of the entire molecule because data collected up to now are not conclusive to assign an oxidation state to the iron metal of the supposed carbene species. As described above, we can confidently suggest that the axial methoxy ligand was not lost during the cyclopropanation in accord with the Fe(**2**)(OMe) recovery at the end of the catalytic reaction.

The determination of the preferred binding mode and spin state of the carbene intermediates **X** and **Y** started with the study of unsubstituted porphyrin **21**, which shows hydrogen atoms on all the *meso*-positions (namely porphine). Figure 5 reports their optimized structures together with the transition state interconverting them. The calculations showed that the *bridging* mode **21Y** is more stable than the *terminal* mode **21X** by > 20 kcal/mol, contrarily to other iron porphyrin carbenes reported in literature.[59] Moreover, whereas **21X** largely prefers the lowest doublet spin state (S = 1/2), in **21Y** the quartet spin state (S = 3/2) is preferred by 7-8 kcal/mol over the doublet and sextet spin states. When the transition state for their interconversion was located and optimized at the three possible spin states, it was shown to be geometrically and electronically very close to the *terminal* carbene **21X** with a defined preference for the doublet spin state. An examination of the spin density distribution shows that it is essentially located onto iron and the oxygen and carbon atoms linked to it. This holds true in both the carbene intermediates, in spite of their different spin state with the obvious difference of the much higher spin density on iron in the *bridging* intermediate **21Y** (Table 1S, SI). However, the Fe-C bond length is significantly different being 1.85 Å in **21X** and 2.03 Å in **21Y** in agreement with its double and single bond character, respectively. As far as the charge distribution is concerned, positive and negative charges were found on the iron and carbene carbon atoms, respectively, greater in **21Y** and smaller in **21X** (Table S1, SI).

In principle, the geometrical constraints given by the *meso*-phenyls, the pickets, and the binaphthyl moieties might alter the relative stability of intermediates **21X** (*terminal*) and **21Y** (*bridging*) so that it is mandatory to evaluate the relative energy of the different carbene binding modes on the intermediates obtained from Fe(**19**)(OMe) and Fe(**20**)(OMe). In both the cases, results very similar to those obtained with unsubstituted porphyrin were obtained, indicating both a greater stability of the *bridging* carbene and a general preference of the *terminal* carbene species for the doublet spin state (see SI).

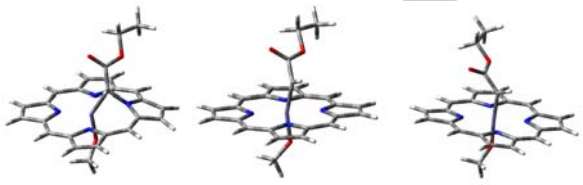

bridging (**21Y**) TS *terminal* (**21X**)

Figure 5. Three-dimensional plot of the *terminal* **21X** and *bridging* **21Y** carbene deriving from the EDA attack to the unsubstituted porphyrin together with the transition state for their interconversion.

When the carbene intermediate reacts with α-methylstyrene, the *trans* cyclopropane compound was obtained with excellent diastereoselectivity and good enantioselectivity in the reaction catalysed by Fe(**2**)(OMe). This means that the four possible approaches of the alkene to the carbene species have different probability to occur, being the two approaches yielding the *trans* adduct energetically favoured over those yielding the *cis* adduct. The determination of the geometry and energy of the four corresponding transition states could give reason of the observed selectivities.

Before facing the problem of locating these transition states on the very large structure including the Fe(**20**)(OMe)-carbene complex and α-methylstyrene, we considered systems of initially lower but successively increasing complexity. First, the transition state for addition of ethylene to the carbene deriving from the attack of EDA to unsubstituted iron porphyrin **21** was located in the three possible spin states and, once again, the doublet spin state was shown to be preferred by 11-12 kcal/mol. So, in all the following studies, only the doublet state was considered for all the transition states under investigation. It is worthy pointing out that, in spite of the negative charge located on the carbene carbon atom of intermediates **21X** and **21Y**, a charge transfer of 0.128 *e* from ethylene to the iron complex was observed in the transition state, supporting the electrophilic reactivity of the carbene intermediate.[78]

Then, we located the two transition states for the *trans* and *cis end-on* attack of α-methylstyrene to a carbene species deriving from Fe(TPP)(OMe) (TPP = dianion of tetraphenyl porphyrin) which lacks the pickets and binaphthyl units. Intermediate Fe(TPP)(OMe)(CHCOOEt) was considered the minimum structure able, on geometrical grounds, to furnish significant information to be transferred to the complete structure. The two transition states reported in Figure 6 were located. The *trans*-TS resulted more stable by 0.91 kcal/mol than the *cis*-TS. They both showed a very asynchronous but concerted formation of the two

new C-C bonds of cyclopropane without observation of any intermediate radical species in which a new C-C bond is completely formed and the other one is not.

IRC calculations were performed starting from the two *trans* and *cis* transition states in both the forward and reverse directions. In the forward direction the transition states were directly connected to the cyclopropane adducts and in the reverse direction the transition states go back to α-methylstyrene and *terminal* carbene reagents. These results suggested that the *terminal* carbene should be the active catalytic species and thus the attack to the alkene must be preceded by the conversion of the carbene from the *bridging* to the *terminal* mode.

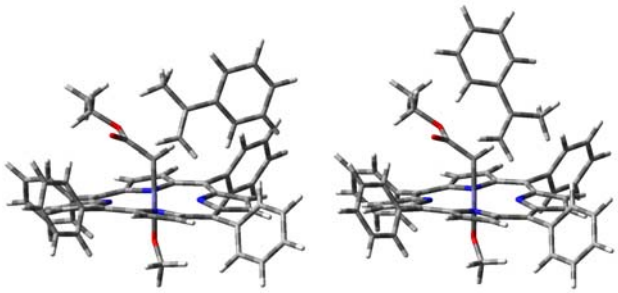

trans-TS (0.00) *cis*-TS (0.91)

Figure 6. Three-dimensional plot of the transition states for the attack of α-methylstyrene to the terminal carbene species deriving from Fe(TPP)(OMe) (relative energy values, kcal/mol, in parentheses).

Finally, the handle of **20** in the **20A-D** geometry was built around the two above *trans* and *cis*-TSs. Each of them was used twice, as such and as the mirror image, in order to obtain four TS starting geometries able to furnish the four (1*R*,2*R*), (1*S*,2*S*), (1*R*,2*S*), and (1*S*,2*R*) stereoisomeric cyclopropane reaction products.

After a considerable computational effort, the four TSs were optimized. Their three-dimensional plots are reported in Figure 7. In very good agreement with the observed selectivity, the two *trans*-TSs resulted significantly more stable than the two *cis*-TSs whereas a small energy difference was found between the two *trans*-TSs, so justifying the observed good but not excellent enantioselectivity.

The plots in Figure 7 show that in the *trans*-TSs the styrene phenyl group points away from catalytic site whereas in the *cis*-TSs it points towards the crowded region between the phenyls of the pickets up to be close to the methoxy naphthyl groups, suggesting a geometrical explanation for the excellent diastereoselectivity observed in the Fe(**2**)(OMe) catalysed cyclopropanation reaction.

The chiral binaphthyl group that, in **2**, functionalises the benzylic groups of the two arms of porphyrin **1**, represents a ceiling quite distant from the catalytic site, so being unable to produce a complete differentiation of the enantiomeric reaction paths. Moreover, it does not freeze in a rigid orientation the lateral pickets so that the cavity remains able to accommodate guests of different size, shape and chirality by an easy lateral movements of the pickets, as described above for **20**.

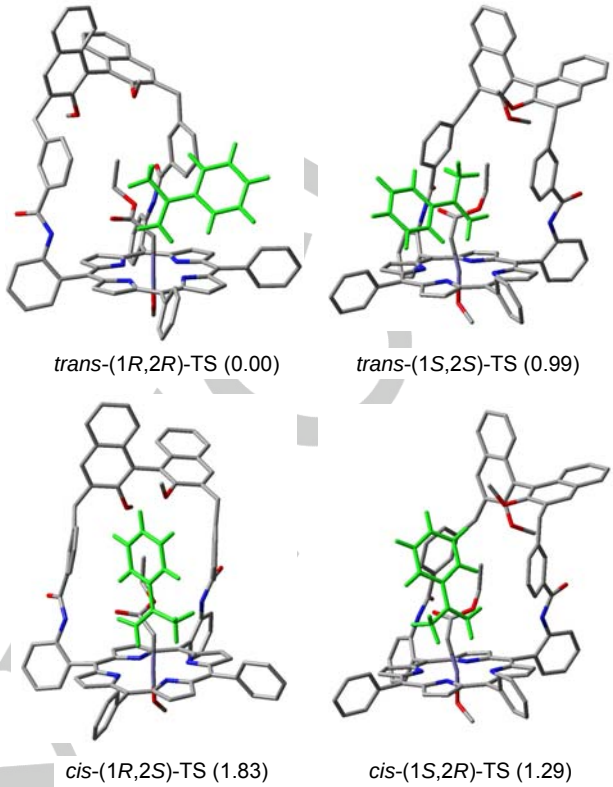

trans-(1*R*,2*R*)-TS (0.00) *trans*-(1*S*,2*S*)-TS (0.99)

cis-(1*R*,2*S*)-TS (1.83) *cis*-(1*S*,2*R*)-TS (1.29)

Figure 7. Transition states for the end-on attack of α-methylstyrene to the terminal carbene-porphyrin deriving from Fe(**20**)(OMe) (relative energy values, kcal/mol, in parentheses). The hydrogen atoms of the carbene iron complex are omitted for clarity. All the atoms of α-methylstyrene are shown in green.

Conclusions

In summary, we have reported a synthetic approach affording a modular chiral porphyrin constituted by three different portions, which separately contribute to the stereoselective promotion of alkene cyclopropanations. The bottom of the '*totem*' porphyrin is represented by the N_4 tetrapyrrolic unit containing the catalytically active iron metal centre, responsible for the diazo compound activation. Then, the functionalization of the *αααβ*-tetraamino tetraphenyl porphyrin permitted the building of a C_2 symmetrical porphyrin skeleton which was very efficient in inducing high *trans*-diasteromeric ratios. Finally, the further improvement of the diastereoselectivity and the reaction enantioselectivity was due to the introduction of a chiral '*hat*' onto the C_2 symmetrical structure. The so-obtained chiral '*totem*' porphyrin catalysed the cyclopropantion of several alkenes with high TON and TOF values (up to 10,000 and 120,000 h^{-1}, respectively) and by using differently encumbered monosubstituted diazo derivatives of the general formula $(RO_2C)CHN_2$. Reactions were generally very fast and occurred with *trans*/*cis* diasteroselectivity ratios up to 99:1 and enantioselectivity of the *trans*-isomer up to 87%.

In order to shed light on the reasons that influence the selectivity, attention was focused on the mechanism of the

carbene transfer reaction promoted by Fe(**2**)(OMe) through a DFT study. The theoretical investigation suggested, in accord with experimental data, the involvement of an iron carbene intermediate bearing a methoxy axial ligand in the *trans* position with respect to the active carbene functionality. The optimization of transition states of the approach of α-methylstyrene to carbene intermediate revealed a higher stability of the *trans*-TSs, in agreement with the experimental results on the large preference for the *trans*-cyclopropane adducts. In addition, the calculated small energy difference between the two *trans*-TSs explained the non-perfect differentiation of the two enantiomeric pathways, giving reason for the not so high enantioselectivity observed for all the tested substrates.

It is important to point out that data reported in the present manuscript represent the starting point to build a small library of C_2 symmetrical chiral catalysts where different chiral groups will be introduced as the *'totem hat'*. A correct design of new chiral catalysts will have to be sustained and guided by modeling studies that have demonstrated, in the present case, a nice correlation with the experimental data.

Experimental Section

General Conditions. Unless otherwise specified, all reactions were carried out under nitrogen atmosphere employing standard Schlenk techniques and magnetic stirring. Anhydrous solvents (*n*-hexane, THF, benzene, toluene and dichloromethane) were purified by using standard procedures.

Reagents. Alkenes were purified by using standard procedures and stored under nitrogen. (*R*)-2,2'-dimethoxy-1,1'-binaphthyl-3,3'-diboronic acid,[79] and porphyrin **1**[80] were synthesised by methods reported in the literature or by using minor modifications of them. Diazo compounds were synthesised by modifying the procedure reported by Fukuyama[81] (see SI for details) and analytical data are in accordance with reported data.[81, 82] All the other starting materials were commercial products used as received. Analytical data of cyclopropanes **3**-**10**,[65, 69, 83, 84] **12**,[83] **16**[85] and **17**,[86] were in accordance with reported data (see SI for details) .

Instruments. NMR spectra were recorded at room temperature on a Bruker Avance 300-DRX, operating at 300 MHz for ^{1}H, at 75 MHz for ^{13}C and at 282 MHz for ^{19}F, or on a Bruker Avance 400-DRX spectrometers, operating at 400 MHz for ^{1}H, at 100 MHz for ^{13}C and 376 MHz for ^{19}F, or on a Bruker Avance 500-DRX spectrometer operating at 500 MHz for ^{1}H and at 125 MHz for ^{13}C. Chemical shift (ppm) are reported relative to TMS. The ^{1}H NMR signals of the compounds described in the following have been attributed by 2D NMR techniques. Assignments of the resonance in ^{13}C NMR were made by using the APT pulse sequence and HSQC and HMBC techniques. GC-MS analyses were performed on Shimadzu QP5050A instrument. Infrared spectra were recorded on a Varian Scimitar FTS 1000 spectrophotometer. UV/Vis spectra were recorded on an Agilent 8453E instrument. $[\alpha]_D$ values are given in 10^{-1}deg cm^2 g^{-1}. The ESR spectra were recorded from a sample powder at 77 K with a Bruker EMX X-band spectrometer equipped with an Oxford cryostat. Elemental analyses and mass spectra were recorded in the analytical laboratories of Milan University.

Synthesis of compound Fe(1)(OMe). In a dried 50 mL Schlenk flask, compound **1**[80] (0.080 g, 6.22×10^{-5} mol) and $FeBr_2$ (0.134 g, 6.22×10^{-4} mol) were dissolved in 25.0 mL of THF. The dark solution was refluxed for 7 hours until the complete consumption of **1** that was monitored by TLC. The mixture was evaporated to dryness and the residue purified by chromatography (alumina 0.063-0.200 mm, CH_2Cl_2/CH_3OH 99.8:0.2). (0.083 g, 97%). IR (CH_2Cl_2): ν 3421.3 (w), 2963.1 (w), 2927.5 (w), 2854.9 (w), 1740.1 (w), 1680.0 (w), 1582.2 (w), 1518.0 (w), 1448.3 (w), 1306.9 (w), 1259.9 (w) cm^{-1}. IR (ATR): ν 3413.8 (w), 2961.7 (w), 2925.6 (w), 2853.4 (w), 1731.4 (w), 1672.0 (w), 1578.8 (w), 1510.7 (w), 1442.2 (w), 1300.2 (w), 1257.9 (w), 1081.6 (w), 1014.0 (w), 795.0 (w) cm^{-1}. UV-Vis (CH_2Cl_2): λ_{max} (*log* ε) = 420 (5.16), 620 (4.62) nm. High spin S = 5/2 was confirmed by the g tensor values ($g_\perp$ = 5.7 and $g_{//}$ = 2.00). ESI-MS: *m/z* = 1392.2 [M+Na$^+$]. Elemental analysis calcd (%) for $C_{77}H_{55}Cl_4FeN_8O_5$: C, 67.51; H, 4.05; N, 8.18; O, 5.84. Found: C, 67.26; H, 4.27; N, 8.20.

Synthesis of porphyrin 2. In a dried 100 mL Schlenk flask, compound **1**[80] (0.300 g, 2.33×10^{-4} mol), (*R*)-2,2'-dimethoxy-1,1'-binaphthyl-3,3'-diboronic acid (0.226 g, 5.60×10^{-4} mol), *tetrakis*(triphenylphosphine)palladium(0) (0.108 g, 9.34×10^{-5} mol) and potassium carbonate (0.516 g, 3.71×10^{-3} mol) were dissolved in 16.0 mL of toluene, 5.0 mL of ethanol and 8.0 ml of water. The biphasic solution was refluxed for 4 hours until the complete consumption of **1** that was monitored by TLC. The resulting mixture was allowed to reach room temperature and the biphasic solution was diluted with 50.0 mL of saturated aqueous NH_4Cl and 50.0 mL of CH_2Cl_2 and then it was separated. The aqueous phase was extracted with an additional 2×50 mL of CH_2Cl_2, and the combined organic phases were washed with 1×50 mL of water and 1×50 mL of saturated aqueous $NaHCO_3$. The organic phase was dried over Na_2SO_4 and filtered. The filtrate was concentrated *in vacuo* and then purified by chromatography (silica gel 15-40 μm, CH_2Cl_2/MeOH 99.5:0.5). (0.143 g, 35%). $[\alpha]_D^{20}$ = -809.524 (c=7×10^{-4} g/100mL; in CH_2Cl_2); ^{1}H NMR (500 MHz, $CDCl_3$, 298 K): δ 9.07 (2H, d, $^3J_{HH}$ = 8 Hz, $H_{meso\text{-}Ar}$), 9.00 (2H, s, $H_{\beta pyr}$), 8.95 (2H, s, $H_{\beta pyr}$), 8.94 (2H, d, $^3J_{HH}$ = 4 Hz, $H_{\beta pyr}$), 8.90 (2H, d, $^3J_{HH}$ = 8 Hz, $H_{meso\text{-}Ar}$), 8.88 (2H, d, $^3J_{HH}$ = 4 Hz, $H_{\beta pyr}$), 7.98 (2H, dd, $^1J_{HH}$ = 1 Hz, $^2J_{HH}$ = 8 Hz, $H_{meso\text{-}Ar}$), 7.89 (2H, dt, $^1J_{HH}$ = 1 Hz, $^2J_{HH}$ = 8 Hz, $H_{meso\text{-}Ar}$), 7.86 (2H, dt, $^1J_{HH}$ = 1 Hz, $^2J_{HH}$ = 8 Hz, $H_{meso\text{-}Ar}$), 7.85 (2H, s, NHCO), 7.83 (2H, dd, $^1J_{HH}$ = 1 Hz, $^2J_{HH}$ = 8 Hz, $H_{meso\text{-}Ar}$), 7.70 (4H, d, $^3J_{HH}$ = 8 Hz, $H_{Ar\text{-}binap}$), 7.64 (2H, s, $H_{Ar\text{-}binap}$), 7.63 (2H, s, $H_{Ar\text{-}binap}$), 7.62 (2H, s, NHCO), 7.51 (2H, dt, $^1J_{HH}$ = 1 Hz, $^2J_{HH}$ = 8 Hz, $H_{meso\text{-}Ar}$), 7.49 (2H, dt, $^1J_{HH}$ = 1 Hz, $^2J_{HH}$ = 8 Hz, $H_{meso\text{-}Ar}$), 7.32 (2H, s, $H_{Ar\text{-}strap}$), 7.27 (2H, m, $H_{Ar\text{-}binap}$), 7.19 (2H, s, $H_{Ar\text{-}strap}$), 7.07 (2H, m, $H_{Ar\text{-}binap}$), 6.90 (2H, d, $^3J_{HH}$ = 8 Hz, $H_{Ar\text{-}binap}$), 6.83 (2H, d, $^3J_{HH}$ = 8 Hz, $H_{Ar\text{-}binap}$), 6.67 (2H, d, $^3J_{HH}$ = 8 Hz, $H_{Ar\text{-}strap}$), 6.39 (2H, d, $^3J_{HH}$ = 8 Hz, $H_{Ar\text{-}strap}$), 6.12 (2H, t, $^3J_{HH}$ = 8 Hz, $H_{Ar\text{-}strap}$), 5.98 (2H, t, $^3J_{HH}$ = 8 Hz, $H_{Ar\text{-}strap}$), 5.91 (2H, d, $^3J_{HH}$ = 8 Hz, $H_{Ar\text{-}strap}$), 5.78 (2H, d, $^3J_{HH}$ = 8 Hz, $H_{Ar\text{-}strap}$), 3.87 (2H, d, $^3J_{HH}$ = 8 Hz, CH_2), 3.72 (2H, d, $^3J_{HH}$ = 8 Hz, CH_2), 3.66 (2H, d, $^3J_{HH}$ = 8 Hz, CH_2), 3.55 (2H, d, $^3J_{HH}$ = 8 Hz, CH_2), 2.42 (6H, s, (OMe)), 1.89 (6H, s, (OMe)), -2.64 ppm (2H, s, NH_{int}). ^{13}C NMR (125 MHz, $CDCl_3$, 298 K): δ 166.3, 165.6, 154.9(0), 154.8(7), 141.8, 141.5, 138.9, 138.6, 135.4, 135.2, 135.1, 134.2, 133.5, 133.4, 133.0, 132.6, 131.9, 130.9, 130.4(5), 130.4(2), 130.3(9) (2C), 130.3(5) (2C), 130.1, 128.1, 128.0, 127.7, 127.5(3), 127.4(9), 127.4(3), 126.3, 125.7(5), 125.4(4), 125.4(2), 125.1, 124.9, 124.1, 123.1, 122.8, 122.6, 120.6, 115.6, 115.0, 59.9, 59.8, 38.5, 37.9 ppm. IR (CH_2Cl_2): 3685.7 (w), 3412.8 (w), 1711.0 (w), 1676.8 (w), 1519.1 (w), 1445.1 (w), 1418.5 (w), 1359.6 (w), 1305.9 (w), 1240.9 (w), 1101.2 (w), 1009.5 (w) cm^{-1}. IR (ATR): 3423.6 (w), 3316.6 (w), 3056.6 (w), 2963.2 (w), 2938.3 (w), 1681.2 (w), 1580.8 (w), 1513.1(w), 1443.3 (w), 1302.5 (w), 1260.6 (w), 1101.6 (w) 1012.3 (w) cm^{-1}. UV-Vis (CH_2Cl_2): λ_{max} (*log* ε) = 423 (4.82), 517 (3.57), 551 (3.06), 590 (2.96), 646 (2.71) nm. ESI-MS: *m/z* = 1767.1 [M$^+$]. Elemental analysis calcd (%) for $C_{120}H_{86}N_8O_8$: C, 81.52; H, 4.90; N, 6.34. Found: C, 81.26; H, 4.97; N, 5.94.

Synthesis of complexes Fe(2)(OMe). In a dried 50 mL Schlenk flask, porphyrin **2** (0.078 g, 4.41×10^{-5} mol) and $FeBr_2$ (0.095 g, 4.40×10^{-4} mol)

were dissolved in 25.0 mL of THF. The dark solution was refluxed for 24 hours until the complete consumption of **2** that was monitored by TLC. The mixture was evaporated to dryness and the residue purified by chromatography (alumina 0.063-0.200 mm, CH_2Cl_2/CH_3OH 99.5:0.5). (0.081 g, 99 %). $[\alpha]_D^{20}$ = -625.000 (c = 8×10^{-4} g/100mL; in CH_2Cl_2). IR (CH_2Cl_2): 3685.7 (w), 3418.9 (w), 1723.7 (w), 1676.8 (w), 1605.3 (w), 1516.9 (w), 1278.4 (w), 1098.0 (w), 1009.5 (w) cm^{-1}. IR (ATR): 3417.6 (w), 2962.0 (w), 2926.0 (w), 2854.1 (w), 1677.1 (w), 1513.6 (w), 1259.2 (w), 1087.3 (w), 1011.4 (w), 795.0 (w) cm^{-1}. UV-Vis (CH_2Cl_2): λ_{max} (*log* ε) = 420 (4.58), 576 (3.35) nm. ESR data (experimental X-band (9.462 GHz) sample powder, 77 K): High spin S = 5/2 was confirmed by the g tensor values ($g_\perp$ = 5.71 and $g_{//}$ = 2.00). ESI-MS: *m/z* = 1875.6 [M+Na^+]. Elemental analysis calcd (%) for $C_{121}H_{87}FeN_8O_9$: C, 78.43; H, 4.73; N, 6.05. Found: C, 78.83; H, 4.65; N, 6.15.

Synthesis of complexes Fe(2)OH. ***Method a.*** In a dried 50 mL Schlenk flask, porphyrin **2** (0.078 g, 4.41×10^{-5} mol) and $FeBr_2$ (0.095 g, 4.40×10^{-4} mol) were dissolved in 25.0 mL of THF. The dark solution was refluxed for 24 hours until the complete consumption of **2** that was monitored by TLC. The mixture was evaporated to dryness and the residue purified by chromatography (alumina 0.063-0.200 mm, CH_2Cl_2). The solid was treated with a water solution of NaOH (18,0 mg of NaOH in 10.0 ml of distilled water) and left for 48 hours at room temperature. The precipitated dark solid was then collected by filtration and dried *in vacuo*. (0.081 g, 99 %). $[\alpha]_D^{20}$ = -625.000 (c = 8×10^{-4} g/100mL; in CH_2Cl_2). IR (CH_2Cl_2): 3416.6 (w), 2961.7 (w), 2929.2 (w), 2855.9 (w), 1730.7 (w), 1677.4 (w), 1603.1 (w), 1516.1 (w), 1241.9 (w), 1099.7 (w), 1010.4 (w) cm^{-1}. IR (ATR): 3419.3 (w), 2960.0 (w), 2922.9 (w), 2854.2 (w), 1679.3 (w), 1511.9 (w), 1258.2 (w), 1079.0 (w), 1011.5 (w), 792.0 (w) cm^{-1}. UV-Vis (CH_2Cl_2): λ_{max} (*log* ε) = 420 (4.68), 577 (3.50) nm. ESR data (experimental X-band (9.462 GHz) sample powder, 77 K): High spin S =-5/2 was confirmed by the g tensor values ($g_\perp$ = 5.71 and $g_{//}$ = 2.00). ESI-MS: *m/z* = 1861.6 [M+Na^+]. Elemental analysis calcd (%) for $C_{120}H_{85}FeN_8O_9$: C, 78.38; H, 4.66; N, 6.09. Found: C, 78.83; H, 4.65; N, 6.12.

Method b. In a one neck 25 mL flask, complex Fe(**2**)(OMe) (10 mg) were dissolved in toluene (5.0 mL) containing 0.03% of water and the resulting solution was stirred at room temperature for 24 h. Then the solvent was evaporated to dryness and the solid dried *in vacuo.* IR (CH_2Cl_2): 3416.6 (w), 2961.7 (w), 2929.2 (w), 2855.9 (w), 1730.7 (w), 1677.4 (w), 1603.1 (w), 1516.1 (w), 1241.9 (w), 1099.7 (w), 1010.4 (w) cm^{-1}. IR (ATR): 3419.3 (w), 2960.0 (w), 2922.9 (w), 2854.2 (w), 1679.3 (w), 1511.9 (w), 1258.2 (w), 1079.0 (w), 1011.5 (w), 792.0 (w) cm^{-1}. UV-Vis (CH_2Cl_2): λ_{max} (*log* ε) = 420 (4.68), 577 (3.50) nm. ESI-MS: *m/z* = 1861.6 [M+Na^+]. Elemental analysis calcd (%) for $C_{120}H_{85}FeN_8O_9$: C, 78.38; H, 4.66; N, 6.09. Found: C, 78.75; H, 4.57; N, 6.22.

General catalytic procedures. The stock solution 5.40 x 10^{-4} mol/L of the catalyst was prepared by dissolving 10,0 mg of Fe(**2**)(OMe) in 10,0 mL of dry toluene or 7,32 mg of Fe(**1**)(OMe) in 10,0 mL of dry toluene or 9,9 mg of Fe(**2**)OH in 10,0 mL of dry toluene. The obtained solution was used for the following catalytic reactions. ***Method a.*** In a typical run, 1.0 mL of the iron catalyst solution was dissolved in 2.0 mL of dry toluene before adding equimolar amounts of the required alkene and diazo compound (5.39×10^{-4} mol) at 25°C. The consumption of diazo compound was monitored by IR spectroscopy by measuring the decrease of the characteristic N_2 absorbance at ≈2110 cm^{-1}. The reaction was considered to be finished when the measured diazo compound absorbance was below 0.03 (by using a 0.5 mm-thickness cell). The solution was then evaporated to dryness and analysed. ***Method b.*** The procedure illustrated for *method a* was repeated by using an alkene/diazo compound molar ratio of 1000:1100 at different temperatures. ***Method c.*** The procedure illustrated for *method a* was repeated by using an alkene/diazo compound molar ratio of 10000:10100 at 0°C. ***Method d:*** Fe(**2**)(OMe) (1.0 mL of the stock solution) was dissolved in 2.0 mL of dry toluene in a flask equipped with a calcium chloride drying tube, then α-methylstyrene and EDA were added with a molar ratio of Fe(**2**)(OMe)/ α-methylstyrene/EDA of 1:1000:1000. ***Method e:*** Fe(**2**)(OMe) (1.0 mL of the stock solution) was dissolved in 2.0 mL of toluene in air and in the presence of activated 4Å molecular sieves. Then α-methylstyrene and EDA were added with a molar ratio of Fe(**2**)(OMe)/ α-methylstyrene/EDA of 1:1000:1000. ***Method f:*** Fe(**2**)(OMe) (1.0 mL of the stock solution) was dissolved in 2.0 mL of dry toluene containing 0.03% of degassed water. Then α-methylstyrene and EDA were added with a molar ratio of Fe(**2**)(OMe)/ α-methylstyrene/EDA of 1:1000:1000.

***Trans* ethyl–2–methyl–2–(4–fluorophenyl)cyclopropanecarboxylate (11).** The crude was purified by flash chromatography (silica gel, AcOEt/^{n}hexane 0.5:9.5) to give a yellow oil. The product was analysed by NMR and HPLC by using a chiral column (DAI–CEL CHIRALCEL, IB, ^{n}hexane/^{i}PrOH = 99.75:0.25). ^{1}H NMR (300 MHz, $CDCl_3$, 300 K): δ 7.36-7.21 (2H, m, H3), 7.01-6.95 (2H, m, H2), 4.29-4.14 (2H, m, H10), 1.93 (1H, m, H8), 1.52 (3H, s, H6), 1.45 (1H, m, H7), 1.42-1.35 (1H, m, H7), 1.33 ppm (3H, t, $^3J_{HH}$ = 7.1 Hz, H11). ^{13}C NMR (75 MHz, $CDCl_3$, 300 K): δ 172.41 (s, C9), 161.8 (d, $^1J_{CF}$ = 244.9 Hz, C1), 142.15 (d, $^4J_{CF}$ = 3.1 Hz, C4), 129.38 (d, $^3J_{CF}$ = 8.1 Hz, C3), 115.59 (d, $^2J_{CF}$ = 21.3 Hz, C2), 60.94 (s, C10), 30.43 (s, C5), 28.16 (s, C8), 21.11 (s, C7), 20.54 (s, C6), 14.79 ppm (s, C11). ^{19}F NMR (282 MHz, $CDCl_3$): δ -116.65 ppm (s). MS (EI): *m/z* 222 [M].

***Trans* ethyl 2–(4–chloromethylphenyl)cyclopropanecarboxylate (13).** The crude was purified by flash chromatography (silica gel, AcOEt/^{n}hexane 1:9) to give a yellow oil. The product was analysed by NMR.^{1}H NMR (300 MHz, $CDCl_3$, 300 K): δ 7.30 (2H, d, $^3J_{HH}$ = 8.1 Hz, H3), 7.09 (2H; d, $^3J_{HH}$ = 8.1 Hz, H4), 4.56 (2H, s, H1), 4.17 (2H, q, $^3J_{HH}$ = 7.1 Hz, H10), 2.61-2.46 (1H, m, H8), 1.89 (1H, ddd, $^3J_{HH}$ = 8.5, 5.3, 4.2 Hz, H6), 1.61 (1H, ddd, $^3J_{HH}$ = 9.2, 5.2, $^2J_{HH}$ = 4.6 Hz, H7), 1.33 (1H, m, H7), 1.28 ppm (3H, t, $^3J_{HH}$ = 7.1 Hz, H11). ^{13}C NMR (75 MHz, $CDCl_3$, 300 K): δ 173.37 (s, C9), 140.73 (s, C5), 135.88 (s, C2), 128.92 (s, C3), 126.70 (s, C4), 60.91 (s, C10), 46.12 (s, C1), 25.99 (s, C6), 24.42 (s, C8), 17.23 (s, C7), 14.40 ppm (s, C11). MS (EI): *m/z* 238 [M].

***Trans* ^{i}propyl–2–methyl–2–phenylcyclopropanecarboxylate (14)**. The crude was purified by flash chromatography (silica gel, AcOEt/^{n}hexane = 0.5:9.5) to give a yellow oil. The product was analysed by NMR and HPLC by using a chiral column (DAI–CEL CHIRALCEL, IB, ^{n}hexane/^{i}PrOH 99.75:0.25). ^{1}H NMR (300 MHz, $CDCl_3$, 300 K): δ 7.34-7.27 (4H, m, H2 e H3), 7.23-7.14 (1H, m, H1), 5.06 (1H, heptet, $^3J_{HH}$ = 6.2 Hz, H10), 1.93 (1H, dd, $^3J_{HH}$ = 8.3, 6.0 Hz, H8), 1.51 (3H, s, H6), 1.42-1.36 (2H, m, H7), 1.26 ppm (6H, d, $^3J_{HH}$ = 6.2 Hz, H11 e H12). ^{13}C NMR (75 MHz, $CDCl_3$, 300 K): δ 171.75 (s, C9), 146.14 (s, C4), 128.55 (s, C2), 127.34 (s, C3), 126.51 (s, C1), 67.88 (s, C10), 30.38 (s, C5), 28.41 (s, C8), 22.26 (s, C11), 22.04 (s, C12), 20.77 (s, C7), 19.89 ppm (s, C6). MS (EI): *m/z* 218 [M].

***Trans* ^{n}propyl–2–methyl–2–phenylcyclopropanecarboxylate (15)**. The crude was purified by flash chromatography (silica gel, AcOEt/^{n}hexane 0.5:9.5) to give a yellow oil. The product was analysed by NMR and HPLC by using a chiral column (DAI–CEL CHIRALCEL, IB, ^{n}hexane/^{i}PrOH = 99.75:0.25). ^{1}H NMR (300 Hz, $CDCl_3$, 300 K): δ 7.28 (4H, dd, $^3J_{HH}$ = 4.4 Hz, H2 e H3), 7.21 (1H, m, H1), 4.10 (2H, t, $^3J_{HH}$ = 6.7 Hz, H10), 1.97 (1H, dd, $^3J_{HH}$ = 8.3, 6.1 Hz, H8), 1.79-1.58 (2H, m, H11), 1.52 (3H, s, H6), 1.48-1.38 (2H, m, H7), 0.97 ppm (3H, t, $^3J_{HH}$ = 7.1 Hz, H11). ^{13}C NMR (75 Hz, $CDCl_3$, 300 K): δ 172.25 (s, C9), 145.96 (s, C4), 128.45 (s, C2), 127.29 (s, C3), 126.44 (s, C1), 66.15 (s, C10), 30.52 (s, C5), 27.90 (s, C8), 22.15 (s, C11), 20.76 (s, C7), 19.93 (s, C6), 10.43 (s, C12). MS (EI): *m/z* 218 [M].

***Trans* 1–phenylpropyl–2–methyl–2–phenylcyclopropanecarboxylate (18).** The crude was purified by flash chromatography (silica gel, AcOEt/^{n}hexane = 0.5:9.5). Two *trans* diasteromers were obtained in mixture and they were analysed by NMR. ^{1}H NMR (400 MHz, $CDCl_3$, 300 K): δ 7.49-7.12 (20H, m, HAr), 5.31-5.01 (2H, m, H10), 3.05-2.88 (2H, m,

H12), 2.86-2.68 (2H, m, H12'), 2.08-1.72 (2H, m, H8), 1.47 (3H, s, $H6_A$), 1.41-1.33 (4H, m, H7), 1.28 (3H, s, $H6_B$), 1.27 (6H, m, H11). ^{13}C NMR (400 MHz, CDCl3, 300 K): δ 171.7 (s), 171.6 (s), 146.2 (s), 146.1 (s), 138 (s), 137.9 (s), 129.6 (d), 128.6 (d), 128.5 (d), 127.57 (s), 127.36 (s), 126.57 (s), 71.89 (s), 71.52 (s), 42.67 (s), 42.47 (s), 30.77 (s), 30.44 (s), 28.37 (s), 28.13 (s), 20.76 (s), 20.36 (s), 20.04 (s), 19.88 (d). MS (EI): *m/z* 294 [M].

Recycle of catalyst Fe(2)(OMe). ***Method a:*** α-Methylstyrene (0.421 mL, 3.24×10^{-3}mol) and EDA (0.340 mL, 3.24×10^{-3}mol) were added to a toluene solution (17.0 mL) of Fe(**2**)(OMe) (6.0 mg, 3.24×10^{-6}mol) at 0°C under nitrogen atmosphere. The consumption of EDA was monitored by IR spectroscopy by measuring the characteristic N_2 absorbance at 2114 cm^{-1}. After the complete EDA consumption, EDA and α-methystyrene were added again to the catalytic mixture for two more consecutive times. The NMR analyses of the crude revealed 90% of global yield, 98% of *trans*-diastereoselectivity with 75% of ee_{trans}. ***Method b.*** Complex Fe(**2**)(OMe) (1.0 mL of the stock solution) was dissolved in 2.0 mL of dry toluene before adding equimolar amounts of α-methylstyrene and EDA (5.39×10^{-4} mol) at 0°C. The consumption of diazo compound was monitored by IR spectroscopy by measuring the decrease of the characteristic N_2 absorbance at 2114 cm^{-1}. After the complete EDA consumption, the solution was evaporated to dryness, the residue was left standing in open air and then analysed. The obtained crude was dissolved in toluene (2.0 mL) and equimolar amounts of α-methylstyrene and EDA (5.39×10^{-4} mol) were added at 0°C. After the complete EDA consumption, the solution was evaporated to dryness and the residue was analysed. This procedure was repeated for another time. ***Method c:*** complex Fe(**2**)(OMe) (1.0 mL of the stock solution) was dissolved in toluene (2.0 mL) and then α-methylstyrene and EDA were added at 0°C with a molar ratio of Fe(**2**)(OMe)/α-methylstyrene/EDA of 1:1000:1100 under nitrogen atmosphere. The consumption of EDA was monitored by IR spectroscopy by measuring the characteristic N_2 absorbance at 2114 cm^{-1}. After the complete EDA consumption, EDA and α-methystyrene were added again to the catalytic mixture for two more consecutive times.

Recovery of catalyst Fe(2)(OMe). In a one neck 25.0 mL flask, complexes Fe(**2**)OH (20.0 mg) were dissolved in dry MeOH (10.0 mL) and the solution was stirred at room temperature overnight; the solvent was then evaporated to dryness and the solid was dried *in vacuo*. IR (CH_2Cl_2): 3685.7 (w), 3418.9 (w), 1723.7 (w), 1676.8 (w), 1605.3 (w), 1516.9 (w), 1278.4 (w), 1098.0 (w), 1009.5 (w) cm^{-1}. IR (ATR): 3417.6 (w), 2962.0 (w), 2926.0 (w), 2854.1 (w), 1677.1 (w), 1513.6 (w), 1259.2 (w), 1087.3 (w), 1011.4 (w), 795.0 (w) cm^{-1}. UV-Vis (CH_2Cl_2): λ_{max} (*log* ε) = 420 (4.58), 576 (3.35) nm. Elemental analysis calcd (%) for $C_{121}H_{87}FeN_8O_9$: C, 78.43; H, 4.73; N, 6.05. Found: C, 78.83; H, 4.65; N, 6.15.

Computational details. All the calculations were carried out using the Gaussian09 program package.[75] After building, all the starting structures were optimized in the gas-phase at the B3LYP/6-31G(d) level[76, 77] for the C, H, N, O atoms. In the case of the metal complexes the effective core potential LanL2DZ was used for the central metal atom to correctly describe the geometries and the electronic properties of compounds containing iron. Optimizations on the doublet (S = 1/2), quartet (S = 3/2), or sextet (S = 5/2) spin states were performed on the iron complexes. Vibrational frequencies were computed at the same level of theory to define the optimized structures as minima or transition states, which present an imaginary frequency corresponding to the forming bonds. NPA charges were determined at the same level of calculations.

Acknowledgements

We wish to thank the Italian MiUR for financial support. Nothing to add??

Keywords: Porphyrin • Iron • Cyclopropanation • Chiral • DFT study

[1] G. Kumari, Nutan, M. Modi, S. K. Gupta, R. K. Singh, *Eur. J. Med. Chem.*, **2011**, *46*, 1181-1188.
[2] A. Reichelt, S. F. Martin, *Acc. Chem. Res.*, **2006**, *39*, 433-442.
[3] F. Gnad, O. Reiser, *Chem Rev*, **2003**, *103*, 1603-1623.
[4] M. P. Doyle, R. Duffy, M. Ratnikov and L. Zhou, *Chem. Rev.*, **2010,** *110*, 704-724.
[5] W. A. Donaldson, *Tetrahedron*, **2001**, *57*, 8589-8627.
[6] L. A. Wessjohann, W. Brandt and T. Thiemann, *Chem. Rev.*, **2003**, *103*, 1625-1648.
[7] P. Tang, Y. Qin, *Synthesis*, **2012**, *44*, 2969-2984.
[8] C. A. Carson, M. A. Kerr, *Chem. Soc. Rev.*, **2009**, *38*, 3051-3060.
[9] H. M. L. Davies, J. R. Denton, *Chem. Soc. Rev.*, **2009**, *38*, 3061-3071.
[10]. H. Lebel, J.-F. Marcoux, C. Molinaro, A. B. Charette, *Chem. Rev.*, **2003**, *103*, 977-1050. .
[11] G. Maas, *Chem. Soc. Rev.*, **2004**, *33*, 183-190.
[12] H. Wang, D. M. Guptill, A. Varela-Alvarez, D. G. Musaev, H. M. L. Davies, *Chem. Sci.*, **2013**, *4*, 2844-2850.
[13] B. Castano, S. Guidone, E. Gallo, F. Ragaini, N. Casati, P. Macchi, M. Sisti, A. Caselli, *Dalton Trans.*, **2013**, *42*, 2451-2462.
[14] A. Caballero, A. Prieto, M. M. Diaz-Requejo, P. J. Perez, *Eur. J. Inorg. Chem.*, **2009**, 1137-1144.
[15] H.-B. Zou, H. Yang, Z.-Y. Liu, M. H. R. Mahmood, G.-Q. Mei, H.-Y. Liu, C.-K. Chang, *Organometallics*, **2015**, *34*, 2791-2795.
[16] A. Ford, H. Miel, A. Ring, C. N. Slattery, A. R. Maguire, M. A. McKervey, *Chem. Rev.*, **2015**, *115*, 9981-10080.
[17] N. M. Roda, D. N. Tran, C. Battilocchio, R. Labes, R. J. Ingham, J. M. Hawkins, S. V. Ley, *Org. Biomol. Chem.*, **2015**, *13*, 2550-2554.
[18] M. I. Burguete, A. Cornejo, E. García-Verdugo, M. J. Gil, S. V. Luis, J. A. Mayoral, V. Martínez-Merino, M. Sokolova, *J. Org. Chem.*, **2007**, *72*, 4344-4350.
[19] S. T. R. Müller, T. Wirth, *ChemSusChem*, **2015**, *8*, 245-250.
[20] B. J. Deadman, S. G. Collins, A. R. Maguire, *Chem. Eur. J.*, **2015**, *21*, 2298-2308.
[21] M. Bordeaux, V. Tyagi, R. Fasan, *Angew. Chem. Int. Ed.*, **2015**, *54*, 1744-1748.
[22] Z. J. Wang, H. Renata, N. E. Peck, C. C. Farwell, P. S. Coelho, F. H. Arnold, *Angew. Chem. Int. Ed.*, **2014**, *53*, 6810-6813.
[23] P. S. Coelho, E. M. Brustad, A. Kannan, F. H. Arnold, *Science*, **2013**, *339*, 307-310.
[24] S. Wallace, E. P. Balskus, *Angew. Chem. Int. Ed.*, **2015**, *54*, 7106-7109.
[25] R. Breslow, *J. Biol. Chem.*, **2009**, *284*, 1337-1342.
[26] P. S. Coelho, Z. J. Wang, M. E. Ener, S. A. Baril, A. Kannan, F. H. Arnold, E. M. Brustad, *Nat Chem Biol*, **2013**, ***9***, 485-487.
[27] M. Otte, P. F. Kuijpers, O. Troeppner, I. Ivanović-Burmazović, J. N. H. Reek, B. de Bruin, *Chem. Eur. J.*, **2014**, ***20***, 4880-4884.
[28] M. Yoshizawa, M. Tamura, M. Fujita, *Science*, **2006**, **312**, 251-254.
[29] M. Otte, P. F. Kuijpers, O. Troeppner, I. Ivanović-Burmazović, J. N. H. Reek, B. de Bruin, *Chem. Eur. J.*, **2013**, ***19***, 10170-10178.
[30] T. Yamaguchi, M. Fujita, *Angew. Chem. Int. Ed.*, **2008**, ***47***, 2067-2069.
[31] K.-H. Chan, X. Guan, V. K.-Y. Lo, C.-M. Che, *Angew. Chem. Int. Ed.*, **2014**, ***53***, 2982-2987.
[32] C.-Y. Zhou, J.-S. Huang, C.-M. Che, *Synlett*, **2010**, 2681-2700.
[33] C.-M. Ho, J.-L. Zhang, C.-Y. Zhou, O.-Y. Chan, J. J. Yan, F.-Y. Zhang, J.-S. Huang, C.-M. Che, *J. Am. Chem. Soc.*, **2010**, *132*, 1886-1894.

[34] Q.-H. Deng, J. Chen, J.-S. Huang, S. S.-Y. Chui, N. Zhu, G.-Y. Li, C.-M. Che, *Chem.-Eur. J.*, **2009**, *15*, 10707-10712.

[35] J.-P. Djukic, D. A. Smith, V. G. Young, Jr., L. K. Woo, *Organometallics*, **1994**, *13*, 3020-3026.

[36] D. A. Smith, D. N. Reynolds, L. K. Woo, *J. Am. Chem. Soc.*, **1993**, *115*, 2511-2513.

[37] C. F. Gorin, E. S. Beh, Q. M. Bui, G. R. Dick, M. W. Kanan, *J. Am. Chem. Soc.*, **2013**, *135*, 11257-11265.

[38] M. L. Rosenberg, K. Vlasana, G. N. Sen, D. Wragg, M. Tilset, *J. Org. Chem.*, **2011**, *76*, 2465-2470.

[39] T. Niino, M. Toganoh, B. Andrioletti, H. Furuta, *Chem. Commun.*, **2006**, 4335-4337.

[40] B. J. Anding, A. Ellern, L. K. Woo, *Organometallics*, **2012**, *31*, 3628-3635.

[41] A. R. Reddy, F. Hao, K. Wu, C.-Y. Zhou, C.-M. Che, *Angew. Chem. Int. Ed.*, **2016**, *55*, 1810-1815.

[42] X. Xu, S. Zhu, X. Cui, L. Wojtas, X. P. Zhang, *Angew. Chem. Int. Ed.*, **2013**, *52*, 11857-11861.

[43] D. Intrieri, A. Caselli, E. Gallo, *Eur. J. Inorg. Chem.*, 2011, 5071-5081.

[44] H. Lu, W. I. Dzik, X. Xu, L. Wojtas, B. de Bruin, X. P. Zhang, *J. Am. Chem. Soc.*, **2011**, *133*, 8518-8521.

[45] A. Penoni, R. Wanke, S. Tollari, E. Gallo, D. Musella, F. Ragaini, F. Demartin, S. Cenini, *Eur. J. Inorg. Chem.*, **2003**, 1452-1460.

[46] E. Rose, N. Raoul, E. Gallo, *J. Porphyrins Phthalocyanines*, **2011**, *15*, 602-611.

[47] G. Du, B. Andrioletti, E. Rose, L. K. Woo, *Organometallics*, **2002**, *21*, 4490-4495.

[48] T.-S. Lai, F.-Y. Chan, P.-K. So, D.-L. Ma, K.-Y. Wong, C.-M. Che, *Dalton Trans.*, **2006**, 4845-4851.

[49] B. Morandi, A. Dolva, E. M. Carreira, *Org. Lett.*, **2012**, *14*, 2162-2163.

[50] B. Morandi, E. M. Carreira, *Science*, **2012**, *335*, 1471-1474.

[51] J. Kaschel, T. F. Schneider, D. B. Werz, *Angew. Chem. Int. Ed.*, **2012**, *51*, 7085-7086.

[52] I. Nicolas, P. L. Maux, G. Simonneaux, *Tetrahedron Lett.*, **2008**, *49*, 5793-5795.

[53] Y. Li, J.-S. Huang, Z.-Y. Zhou, C.-M. Che, X.-Z. You, *J. Am. Chem. Soc.*, **2002**, *124*, 13185-13193.

[54] C. G. Hamaker, G. A. Mirafzal, L. K. Woo, *Organometallics*, **2001**, *20*, 5171-5176.

[55] X. Xu, H. Lu, J. V. Ruppel, X. Cui, S. Lopez de Mesa, L. Wojtas, X. P. Zhang, *J. Am. Chem. Soc.*, **2011**, *133*, 15292-15295.

[56] S. Zhu, X. Xu, J. A. Perman, X. P. Zhang, *J. Am. Chem. Soc.*, **2010**, *132*, 12796-12799.

[57] S. Zhu, J. A. Perman, X. P. Zhang, *Angew. Chem. Int. Ed.*, **2008**, *47*, 8460-8463.

[58] Z. Gross, N. Galili, L. Simkhovich, *Tetrahedron Lett.*, **1999**, *40*, 1571-1574.

[59] R. L. Khade, Y. Zhang, *J. Am. Chem. Soc.*, **2015**, *137*, 7560-7563.

[60] S. Le Gac, B. Boitrel, *New J. Chem.*, **2016**, DOI: 10.1039/C5NJ03120F.

[61] V. Ndoyom, L. Fusaro, T. Roisnel, S. L. Gac, B. Boitrel, *Chem. Commun.*, **2016**, *52*, 517-520.

[62] P. S. Salini, K. S. Anju, M. L. P. Reddy, A. Srinivasan, *Chem. Commun.*, **2013**, *49*, 5769-5771.

[63] D. Savoia, A. Gualandi, *Adv. Org. Synth.*, **2013**, *6*, 167-237.

[64] E. Gallo, E. Rose, B. Boitrel, L. Legnani, L. Toma, *Organometallics*, **2014**, *33*, 6081-6088.

[65] S. Fantauzzi, E. Gallo, E. Rose, N. Raoul, A. Caselli, S. Issa, F. Ragaini, S. Cenini, *Organometallics*, **2008**, *27*, 6143-6151.

[66] E. Rose, N. Raoul, M. Etheve-Quelquejeu, E. Gallo, B. Boitrel, J. Pecaut, L. Dubois, *J. Porphyrins Phthalocyanines*, **2012**, *16*, 324-330.

[67] A. Didier, L. Michaudet, D. Ricard, V. Baveux-Chambenoît, P. Richard, B. Boitrel, *Eur. J. Org. Chem.*, **2001**, 1927-1926.

[68] D. Intrieri, S. Le Gac, A. Caselli, E. Rose, B. Boitrel, E. Gallo, *Chem. Commun.*, **2014**, *50*, 1811-1813.

[69] M. Hagar, F. Ragaini, E. Monticelli, A. Caselli, P. Macchi, N. Casati, *Chem. Commun.*, **2010**, *46*, 6153-6155.

[70] A. M. Harm, J. G. Knight, G. Stemp, *Tetrahedron Lett.*, **1996**, *37*, 6189-6192.

[71] J. R. Wolf, C. G. Hamaker, J.-P. Djukic, T. Kodadek, L. K. Woo, *J. Am. Chem. Soc.*, **1995**, *117*, 9194-9199.

[72] H. M. Mbuvi, L. K. Woo, *Organometallics*, **2008**, *27*, 637-645.

[73] P. Vinš, A. de Cózar, I. Rivilla, K. Nováková, R. Zangi, J. Cvačka, I. Arrastia, A. Arrieta, P. Dražar, J. I. Miranda, F. P. Cossío, *Tetrahedron*, **2016**, *72*, 1120-1131.

[74] I. Artaud, N. Gregoire, P. Leduc, D. Mansuy, *J. Am. Chem. Soc.*, **1990**, *112*, 6899-6905.

[75] Gaussian 09, Revision B.01, M. J. Frisch, G. W. Trucks, H. B. Schlegel, G. E. Scuseria, M. A. Robb, J. R. Cheeseman, G. Scalmani, V. Barone, B. Mennucci, G. A. Petersson, H. Nakatsuji, M. Caricato, X. Li, H. P. Hratchian, A. F. Izmaylov, J. Bloino, G. Zheng, J. L. Sonnenberg, M. Hada, M. Ehara, K. Toyota, R. Fukuda, J. Hasegawa, M. Ishida, T. Nakajima, Y. Honda, O. Kitao, H. Nakai, T. Vreven, J. A. Montgomery, Jr., J. E. Peralta, F. Ogliaro, M. Bearpark, J. J. Heyd, E. Brothers, K. N. Kudin, V. N. Staroverov, T. Keith, R. Kobayashi, J. Normand, K. Raghavachari, A. Rendell, J. C. Burant, S. S. Iyengar, J. Tomasi, M. Cossi, N. Rega, J. M. Millam, M. Klene, J. E. Knox, J. B. Cross, V. Bakken, C. Adamo, J. Jaramillo, R. Gomperts, R. E. Stratmann, O. Yazyev, A. J. Austin, R. Cammi, C. Pomelli, J. W. Ochterski, R. L. Martin, K. Morokuma, V. G. Zakrzewski, G. A. Voth, P. Salvador, J. J. Dannenberg, S. Dapprich, A. D. Daniels, O. Farkas, J. B. Foresman, J. V. Ortiz, J. Cioslowski, D. J. Fox, Gaussian, Inc., Wallingford CT, 2010.

[76] A. D. Becke, *J. Chem. Phys.*, **1993**, *98*, 5648-5652.

[77] C. Lee, W. Yang, R. G. Parr, *Phys. Rev. B*, **1988**, *37*, 785-789.

[78] R. L. Khade, W. Fan, Y. Ling, L. Yang, E. Oldfield, Y. Zhang, *Angew. Chem. Int. Ed.*, **2014**, *53*, 7574-7578.

[79] X.-W. Zou, L.-F. Zheng, L.-L. Wu, L.-L. Zong, Y.-X. Cheng, *Chin. J. Chem* . **2008**, *26,* 373-378.

[80] S. B. Z. Halime, B. Najjari, M. Lachkar, T. Roisnel, B. Boitrel, *J. Porphyrins Phthalocyanines*, **2010**, *14*, 412-420.

[81] T. Toma, J. Shimokawa, T. Fukuyama, *Org. Lett.*, **2007**, *9*, 3195-3197.

[82] D. M. Hodgson, D. Angrish, *Chem. Eur. J.*, **2007**, *13*, 3470-3479.

[83] Y. Chen, X. P. Zhang, *J. Org. Chem.*, **2004**, *69*, 2431-2435.

[84] B. Castano, E. Gallo, D. J. Cole-Hamilton, V. Dal Santo, R. Psaro, A. Caselli, *Green Chemistry*, **2014**, *16*, 3202-3209.

[85] J.-I. Ito, S. Ujiie, H. Nishiyama, *Chem. Eur. J.*, **2010**, *16*, 4986-4990.

[86] S. Ishikawa, R. Hudson, M. Masnadi, M. Bateman, A. Castonguay, N. Braidy, A. Moores, C.-J. Li, *Tetrahedron*, **2014**, *70*, 6162-6168.

Entry for the Table of Contents

FULL PAPER

The activity of chiral Fe(**2**)(OMe) catalyst to promote the cyclopropanation of differently substituted styrenes by diazo derivatives is herein reported. Good stereoselectivities (up to 87% *ee* and 99:1 dr_{trans}) and high TON and TOF values (up to 10,000 and 120,000 h^{-1}, respectively) were achieved. A DFT study was also performed to investigate some mechanistic aspects of the catalytic reaction.

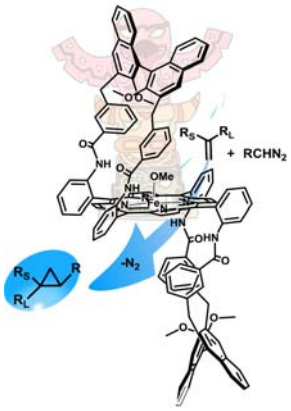

D. M. Carminati, D. Intrieri, A. Caselli, S. Le Gac, B. Boitrel, L. Toma,* L. Legnani and E. Gallo**

Page No. – Page No.

Designing 'Totem' C_2-Symmetrical Iron Porphyrin Catalysts for Stereoselective Cyclopropanations